The RNA-binding protein Musashi1 is a central regulator of adhesion pathways in glioblastoma – supplementary figures and captions

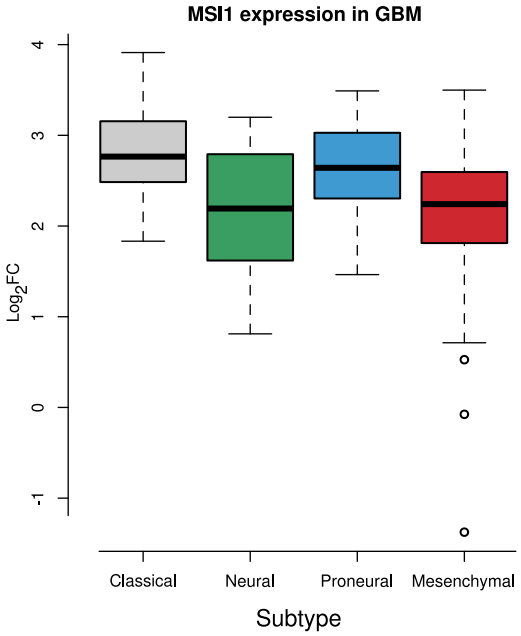

Figure S1

Figure S1: Expression analysis of MSI1 in the TCGA datasets. Box plot showing MSI1 relative gene expression by GBM subtypes, according to TCGA classification: 43 classical samples, 40 proneural samples, 28 neural samples and 56 mesenchymal samples. Data is presented as log2FoldChange, relative to normal brain samples.

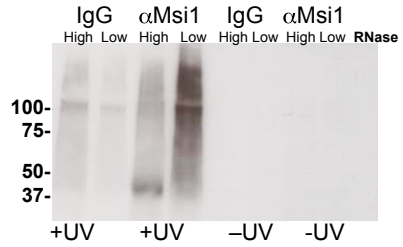

Figure S2

Figure S2: Optimization of iCLIP experiments. We conducted iCLIP experiments in several different conditions using either a-MSI1 or IgG. Results show that the process is specific and good RNA recovery is observed only when a-MSI1 is used and UV crosslinking is performed.

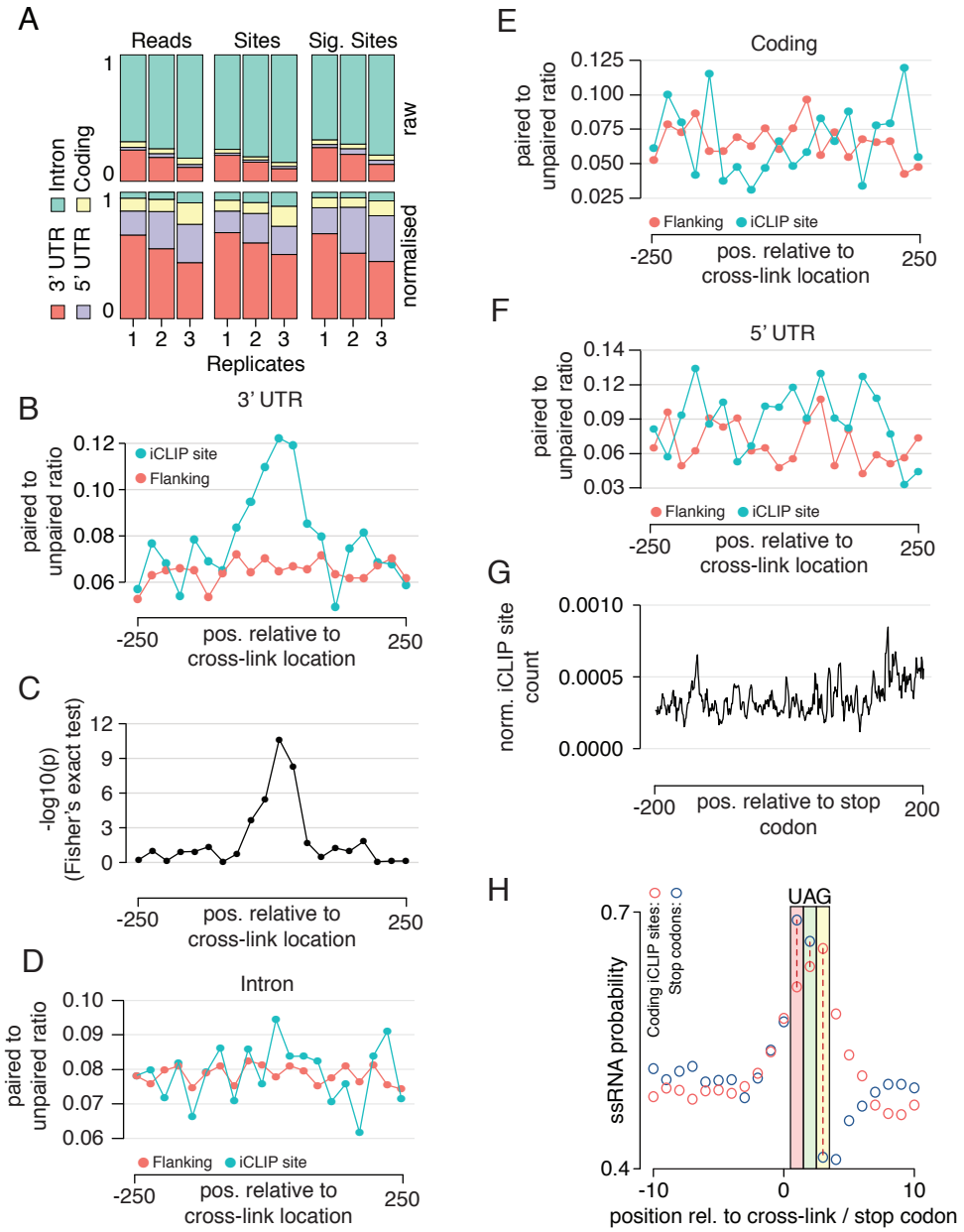

Figure S3

Figure S3: (A) The proportion of raw reads (left), iCLIP sites (middle) and significant iCLIP sites (right) falling within introns, coding regions, 3 UTRs and 5 UTRs. Proportions in the top row are absolute, those in the bottom row are normalized for total region size. (B) Ratio of paired to unpaired UAGs or GUAGs within 250nt of the iCLIP cross-link location and within the 250nt regions immediately flanking; each point represents the ratio of counts in a 25nt window. Only 3 UTR iCLIP sites were used. (C) The p-values from a hyper-geometric test comparing each 25nt window in panel B to the corresponding one in the flanking regions where the null-hypothesis is an odds-ratio of 1. (D) As in panel B, but for intronic sites. (E) As in panel B, but for coding-region sites. (F) As in panel B, but for 5UTR sites. (G) The count of iCLIP sites at each position relative to UAG stop codons, normalized by the total number of positions considered at each relative location. (H) Predicted ssRNA probability around Musashi1 iCLIP sites compared to UAG stop codons.

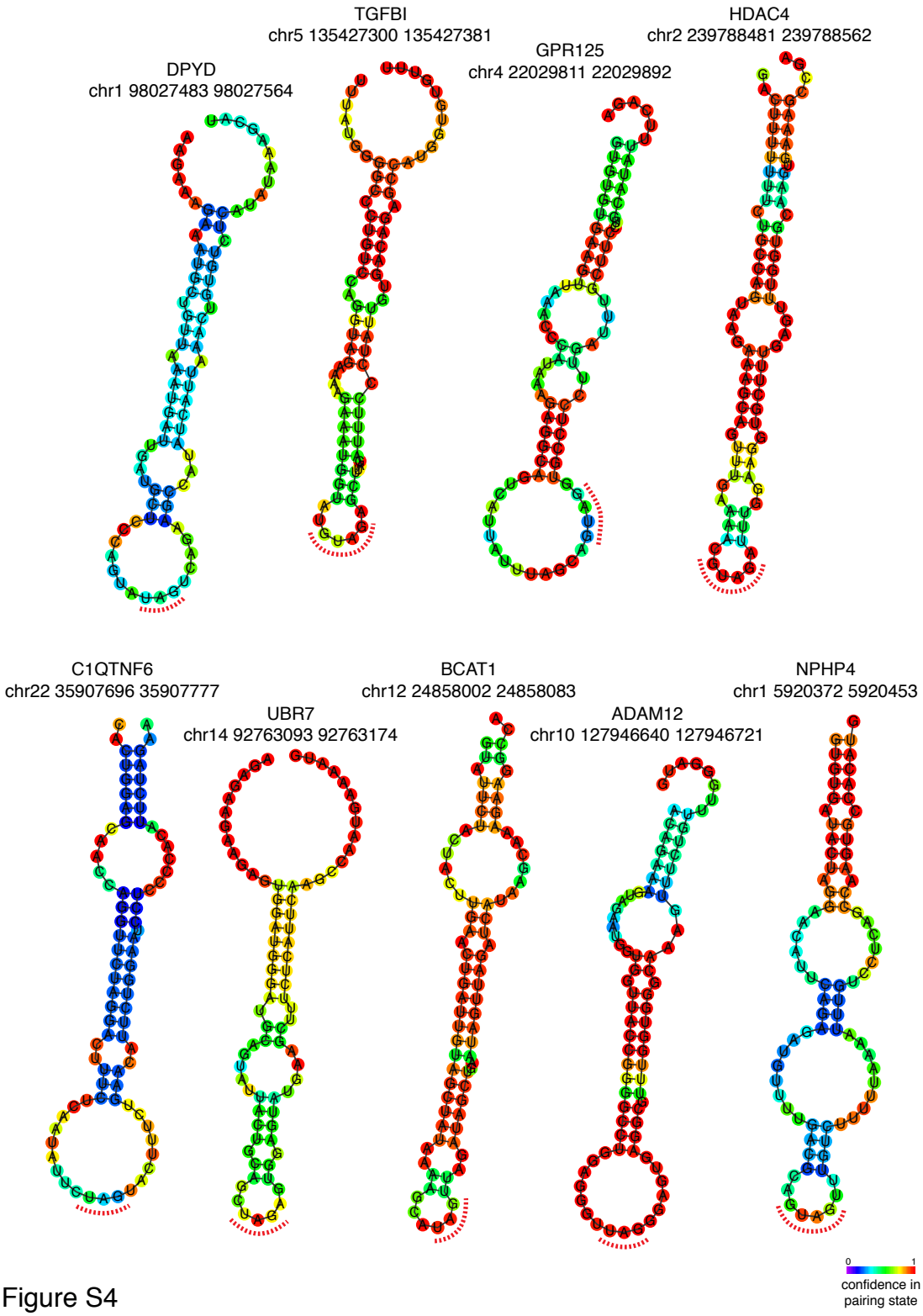

Figure S4

Figure S4: Examples of secondary structures around MSI1 iCLIP sites.

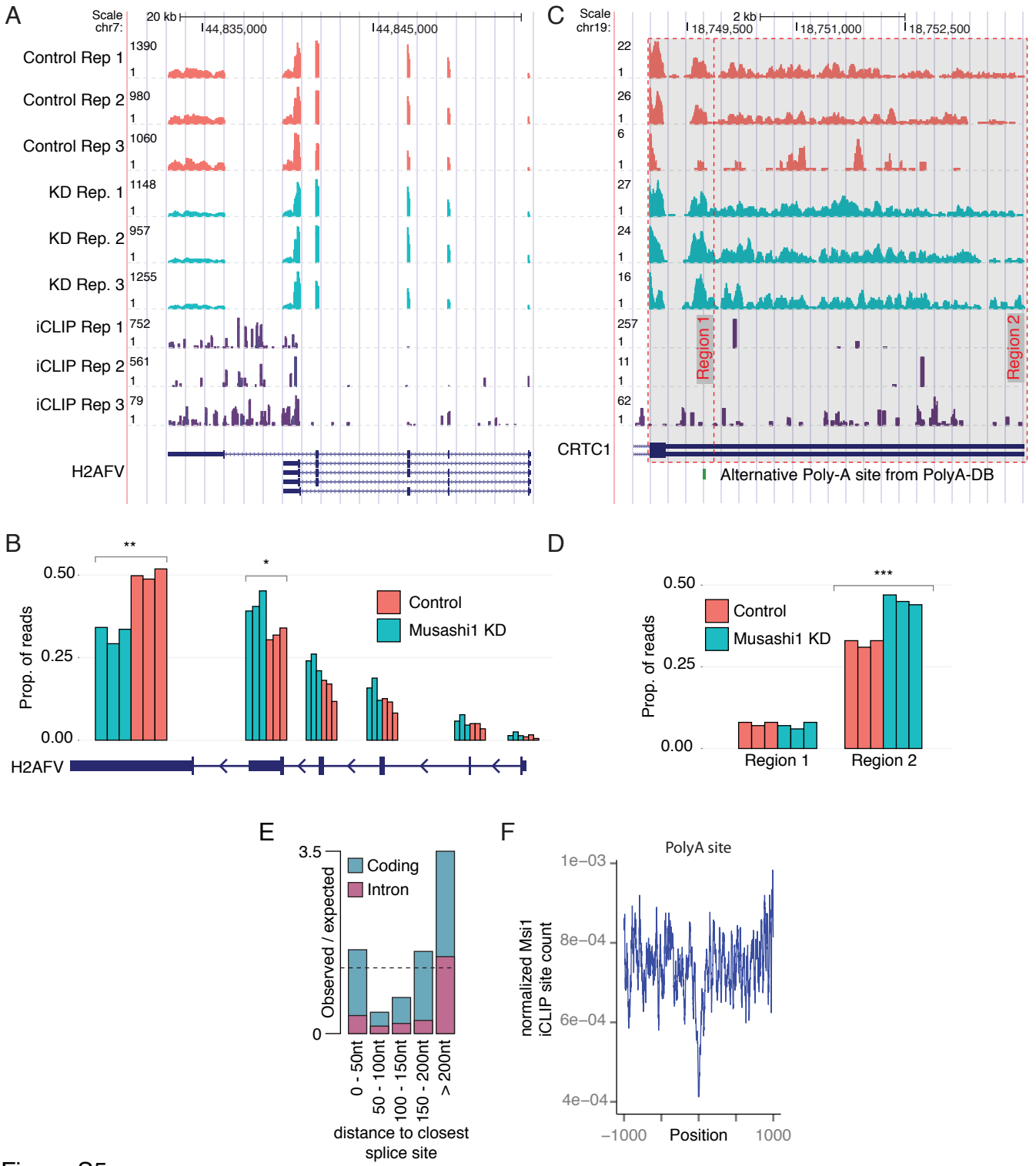

Figure S5

Figure S5: (A) UCSC genome browser image showing RNA-seq read coverage in the three control replicates and three Musashi1 knockdown replicates for the 3 end of the gene H2AFV. Shown also are browser tracks for iCLIP coverage within the same region. (B) A schematic representation of panel A, showing the proportion of reads falling within the gene that are in each of the exons of panel A. (C) As for panel A, but for the gene CRTC1; a change in mRNA levels for the distal portion of the 3 UTR (region 2) after the alternative poly-A site suggests adjusted used of polyadenylation sites. (D) Schematic representation of read coverage in panel C. (E) The observed over expected ratio of counts of coding or intronic iCLIP sites falling within a given distance of a splice site. Expectation is based on random uniform distribution of sites. Dashed line is ratio of 1. (F) Count of Musashi1 iCLIP sites around PolyA signal sites, normalized by the total number of locations considered at each relative distance.

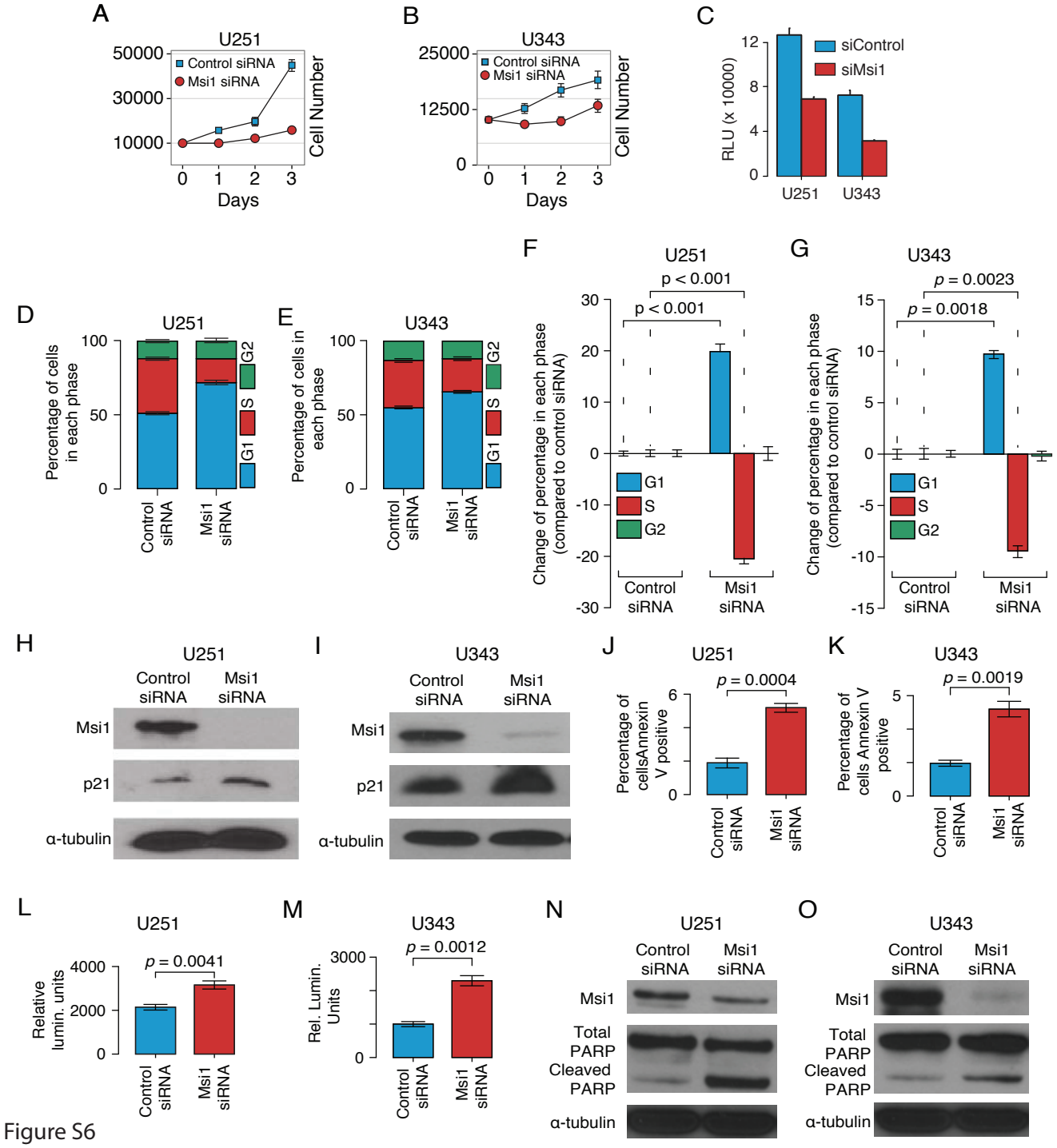

Figure S6

Figure S6: (A and B) Silencing of MSI1 caused a reduction in cell proliferation, determined by cell counting in glioblastoma cells. (C) MSI1 was knocked down in U251 cells and cell viability was determined by CellTiter-Glo luminescent cell viability assay. (D and E) Reduction in MSI1 expression affected cell cycle progression by inducing an accumulation of cells in G1 as compared to the control siRNA transfection in glioblastoma cells. Most of the changes were seen in the redistribution of cells with an increase in cells in G1 phase and decrease in S phase (F and G). Data were analyzed with Students t-test and is presented as the mean standard error of the mean. (H and I) Silencing of MSI1 led to an increase in p21 protein expression as determined by western blot, compared to the control siRNA sample. MSI1 was blotted to confirm silencing, and -tubulin was included as a loading control. (J and K) Reduction of MSI1 expression increased the percentage of Annexin V positive cells, as determined by flow cytometry, in glioblastoma cells (Annexin V is a marker of apoptosis). Data were analyzed with Students t-test and is presented as the mean standard error of the mean. (L and M) Caspase-3/-7 activity, an indicator of apoptosis induction, increased after MSI1 knockdown, as compared to the control siRNA transfection, in glioblastoma cells. Data were analyzed with Students t-test and is presented as the mean standard error of the mean. (N and O) Poly (ADP-ribose) polymerase (PARP), a cleavage target of caspase-3 in vivo, was cleaved upon MSI1 silencing compared to control siRNA, in glioblastoma cells, as detected by western blot using an antibody specific for the full-length and large fragment of PARP. MSI1 is blotted to confirm silencing of MSI1 by siRNA, and -tubulin is included as a loading control.

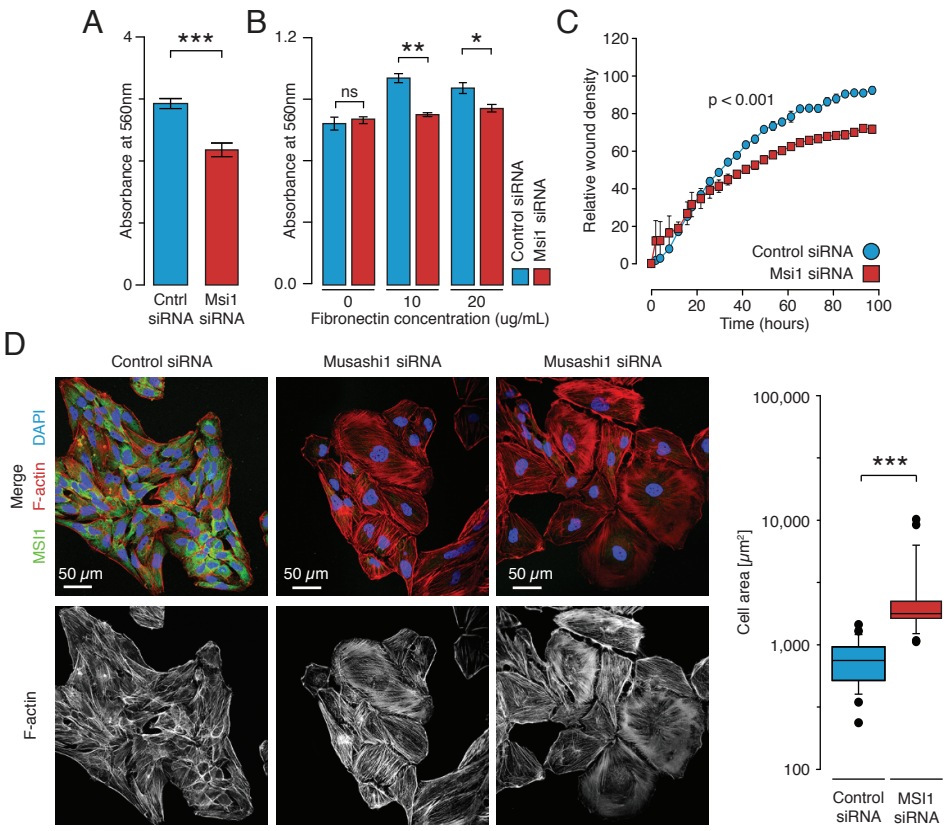

Figure S7

Figure S7: **M**SI1 promotes cell adhesion, migration and invasion in vitro in U343 glioblastoma cells. (A) A colorimetric cell invasion assay was used to determine the effects of MSI1 on the invasiveness of U343 glioblastoma cells through basement membrane. Cells were resuspended in serum-less media, and serum-containing media was used as a chemo-attractant. A basement membrane was used as a barrier between both chambers. After 24 hours of incubation, cells were stained, extracted and quantified. Measuring the extracted cell solution demonstrated that MSI1 silencing impairs in vitro cell invasion, compared to control siRNA transfection. Data were analyzed with Students t-test and is presented as the mean standard error of the mean. (B) A fibronectin cell adhesion assay was employed to determine the effects of MSI1 on cell adhesion in glioblastoma cells. MSI1 silencing reduced the capacity of U343 cells to adhere to the fibronectin substrate. Data were analyzed with Students t-test and is presented as the mean +/- standard error of the mean. (* indicates p value < 0.05, and ** indicates p value < 0.01). (C) In vitro scratch assay was used to assess the effects of MSI1 on the ability for U343 glioblastoma cells to migrate. An IncuCyte automated microscopy system was used to assess scratch wound closure in real time. Data are shown as relative wound density. Data were analyzed with analysis of variance and were presented as the mean standard error of the mean. Silencing of MSI1 resulted in an impairment of wound closure in vitro. (D) Impact of MSI1 silencing on cell morphology was evaluated. U343 cells were transfected with control and MSI1 siRNAs, fixed and processed for indirect immunostaining of MSI1, F-Actin by Phalloidin and nuclei. Representative images are shown. Cell area of transfected cells (n=25) was determined based on F-Actin staining and is shown as box plot (right panels). Bar 25m. Error bars indicated S.d. of at least three independent experiments. ***: $p < 0.001$.